LETTER

IEICE Electronics Express, Vol.14, No.11, 1–10

Total ionizing dose radiation effect on the threshold voltage for the uniaxial strained Si nano NMOSFET

Minru Hao[1a)], **Huiyong Hu**[1], **Chenguang Liao**[1], **Haiyan Kang**[1], **Han Su**[1], **Qian Zhang**[1], **and Yingbo Zhao**[2]

[1] *School of Microelectronics, Xidian University, 2 South Taibai Road, Xi'an 710071, P.R. China*

[2] *Xi'an University of Architecture and Technology, 13 Yanta Road, Xi'an, 710055, P.R. China*

a) *haominru@163.com*

Abstract: The carrier microscopic transport process of uniaxial strained Si n-channel metal-oxide-semiconductor field-effect transistor (NMOSFET) has been analyzed under γ-ray radiation. The variation of oxide-trapped charge (N_{ot}) and interface-trap charge (N_{it}) with the total dose has also been investigated. A two-dimensional analytical model of threshold voltage (V_{th}) has been developed with the degradation due to the total dose irradiation taken into consideration. Based on this model, numerical simulation has been carried out by Matlab, and the influence of the total dose, geometry and physics parameters on threshold voltage (V_{th}) were simulated. In addition, to evaluate the validity of the model, the simulation results were compared with experimental data, and good agreements were confirmed. Thus, the proposed model provides good reference for research on irradiation reliability and application of strained integrated circuit of uniaxial strained Si nanometer n-channel metal-oxide-semiconductor field-effect transistor.

Keywords: uniaxial strained Si, Nano NMOSFET, total dose, threshold voltage (V_{th})

Classification: Electron devices, circuits and modules

References

[1] M. Gaillardin, *et al.*: "Comparative analysis of mechanical strain and silicon film thickness on charge collection mechanisms of nanometer scaled SOI devices under heavy ion and pulsed laser irradiation," IEEE Trans. Nucl. Sci. **61** (2014) 1628 (DOI: 10.1109/TNS.2014.2314143).

[2] Q. Zhou, *et al.*: "Contact resistance reduction for strained N-MOSFETs with silicon-carbon source/drain utilizing aluminum ion implant and aluminum profile engineering," IEEE Trans. Electron Devices **60** (2013) 1310 (DOI: 10.1109/TED.2013.2248367).

[3] W. Wu, *et al.*: "Experimental study on NBTI degradation behaviors in Si pMOSFETs under compressive and tensile strains," IEEE Electron Device Lett. **35** (2014) 714 (DOI: 10.1109/LED.2014.2325032).

DOI: 10.1587/elex.14.20170411
Received April 21, 2017
Accepted April 28, 2017
Publicized May 17, 2017
Copyedited June 10, 2017

[4] A. Abderrahmane, *et al.*: "Proton irradiation enhancement of low-field negative magnetoresistance sensitivity of AlGaN/GaN-based magnetic sensor at cryogenic temperature," IEEE Electron Device Lett. **35** (2014) 1130 (DOI: 10.1109/LED.2014.2358613).
[5] I. S. Esqueda, *et al.*: "Compact modeling of total ionizing dose and aging effects in MOS technologies," IEEE Trans. Nucl. Sci. **62** (2015) 1501 (DOI: 10.1109/TNS.2015.2414426).
[6] E. Garcia-Moreno, *et al.*: "Temperature compensated floating gate MOS radiation sensor with current output," IEEE Trans. Nucl. Sci. **60** (2013) 4026 (DOI: 10.1109/TNS.2013.2277605).
[7] H. Hu, *et al.*: "Novel silicon on insulator monolithic active pixel structure with improved radiation total ionizing dose tolerance and reduced crosstalk between sensor and electronics," IEEE Trans. Nucl. Sci. **62** (2015) 1944 (DOI: 10.1109/TNS.2015.2469534).
[8] T. Kudo, *et al.*: "Development of experimental methodology for highly efficient wafer-level evaluation of X-ray radiation effects on semiconductor devices," IEEE Trans. Nucl. Sci. **61** (2014) 1444 (DOI: 10.1109/TNS.2014.2321766).
[9] H.-Y. Hu, *et al.*: "Study on the influence of γ-ray total dose radiation effect on the threshold voltage and trans-conductance of the strained Si p-channel metal-oxide-semiconductor field-effect transistor," Acta Phys. Sin **63** (2014) 236102 (DOI: 10.7498/aps.63.236102).
[10] J. R. Schwank, *et al.*: "Radiation effects in MOS oxides," IEEE Trans. Nucl. Sci. **55** (2008) 1833 (DOI: 10.1109/TNS.2008.2001040).
[11] C. C. M. Bordallo, *et al.*: "Influence of X-ray radiation on standard and uniaxial strained triple-gate SOI FinFETs," Proc. RADECS (2013) 1 (DOI: 10.1109/RADECS.2013.6937356).
[12] H. Kamimura, *et al.*: "Development of MOS transistors for radiation-hardened large scale integrated circuits and analysis of radiation-induced degradation," J. Nucl. Sci. Technol. **31** (1994) 24 (DOI: 10.1080/18811248.1994.9735112).
[13] F. Stern: "Self-consistent result for N-type Si inversion layers," Phys. Rev. B **5** (1972) 4891 (DOI: 10.1103/PhysRevB.5.4891).
[14] L. D. Yau: "A simple theory to predict the threshold voltage of short-channel IGFET's," Solid-State Electron. **17** (1974) 1059 (DOI: 10.1016/0038-1101(74)90145-2).
[15] K. Suzuki and S. Pidin: "Short-channel single-gate SOI MOSFET model," IEEE Trans. Electron Devices **50** (2003) 1297 (DOI: 10.1109/TED.2003.813450).
[16] V. Kumari, *et al.*: "Analytical modeling of dielectric pocket double-gate MOSFET incorporating hot-carrier-induced interface charges," IEEE Trans. Device Mater. Rel. **14** (2014) 390 (DOI: 10.1109/TDMR.2013.2278077).

1 Introduction

Strained technology has been widely used to improve the performance of Si CMOS devices, and strained-Si technologies have caught much attention as device size is scaling down [1, 2], especially in the applications of strained IC under total dose irradiation. Hence, researches on the irradiated characteristics and the radiation hardening technique are of great significance [3, 4, 5]. A number of articles reported about the electrical characteristics of the MOS device under radiation effect [4, 5, 6, 7, 8]. V_{th}, as an important electrical parameter of a device, has been studied extensively. One-dimensional model on V_{th} of the biaxial strained Si has

DOI: 10.1587/elex.14.20170411
Received April 21, 2017
Accepted April 28, 2017
Publicized May 17, 2017
Copyedited June 10, 2017

been reported before [9]. As devices continue to downscale, their performance cannot be characterized by one-dimensional model of V_{th}. Therefore, a two-dimensional (2D) model needs to be further considered. However, the 2-D model on V_{th} of the uniaxial strained Si nanometer n-channel metal-oxide-semiconductor field-effect transistor (NMOSFET) has rarely been reported.

In this paper, a two-dimensional analytical model on V_{th} of the uniaxial strained Si nanometer NMOSFET was proposed due to the total dose radiation. The results from the model are compared with the experimental data and they are found to be in good agreement. Thus, the model can provide valuable reference for research on irradiation reliability and application of strained integrated circuit of uniaxial strained Si nanometer NMOSFET.

2 Two-dimensional threshold voltage model

The schematic structure of uniaxial strained Si NMOSFET is shown in Fig. 1.

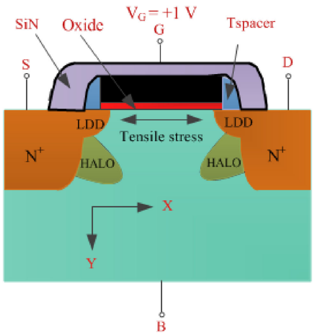

Fig. 1. Structural diagram of uniaxial strained Si nanometer NMOS-FET device.

When the uniaxial strained Si NMOSFET is exposed to γ-ray, electron-hole pairs are created in the oxide. Due to the existence of electric field in gate oxide, as the holes approach the interface, some will be trapped, forming a positive oxide-trap charge. It is believed that hydrogen ions (protons) are likely to be released as holes "hop" through the oxide or as they are trapped near the Si/Oxide interface. The hydrogen ions can also drift to the Si/Oxide where they may react to form interface trap charges [10]. The threshold voltage is affected by both of the above charges, which are expressed as:

$$\frac{\partial P}{\partial t} = k_g f_y D' - \frac{\partial f_p}{\partial x} \tag{1}$$

$$\frac{\partial P_t}{\partial t} = (N_t - P_t)\sigma_{pt} f_p - \frac{P_t}{\tau_t} \tag{2}$$

$$\frac{\partial H^+}{\partial t} = N_{DH}\sigma_{DH} f_p - \frac{\partial f_{H^+}}{\partial x} \tag{3}$$

$$\frac{\partial N_{it}}{\partial t} = (N_{si\text{-}H} - N_{it})\sigma_{it} f_{H^+} - \frac{N_{it}}{\tau_{it}} \tag{4}$$

where p, t and K_g are the hole concentration in the gate dielectric, irradiation time and the number of electron-hole pairs (EHP) generated per unit dose, respectively. f_y, f_p, N_t and p_t are the hole yield as a function of oxide electric, the hole flux,

DOI: 10.1587/elex.14.20170411
Received April 21, 2017
Accepted April 28, 2017
Publicized May 17, 2017
Copyedited June 10, 2017

hole trap concentration and trapped hole concentration in the gate dielectric layer, respectively. σ_{pt}, τ_t, H^+, N_{DH} and σ_{DH} are the hole capture cross section, the annealing time of trap hole respectively, the proton concentration in the oxide layer, the trap concentration of hydrogen and the trapped cross section of holes with hydrogen traps, respectively. $f_H{}^+$, N_{it}, $N_{Si\text{-}H}$ and τ_{it} are the proton flux, the radiation-induced interface defect densities, the silicon dangling bond density of hydrogen passivation and the annealing time of interface traps charge, respectively. The radiation-induced defect densities are quantitative representations of trapped charge integrated across the thickness of the oxide (N_{ot}), and the number of interface traps at the semiconductor/oxide interface (N_{it}). Solving Eqs. (1) (2) (3) and (4), N_{ot} and N_{it} can be obtained as follow:

$$\begin{aligned} N_{ot} &= \frac{1}{t_{ox}}\int_0^{t_{ox}} P_t x dx \\ &= N_t\left[\frac{1}{2}t_{ox} + \frac{e^{-\sigma_{pt}k_g f_y t_{ox} D' t}}{-\sigma_{pt}k_g f_y t_{ox} D' t} + \frac{e^{-\sigma_{pt}k_g f_y t_{ox} D' t} - 1}{(-\sigma_{pt}k_g f_y t_{ox} D' t)^2 t_{ox}}\right] \end{aligned} \tag{5}$$

$$N_{it} = N_{si\text{-}H}(1 - e^{-\sigma_{DH}\sigma_{it}N_{DH}k_g f_y t_{ox}{}^2 D' t}) \tag{6}$$

where the total dose $D = D't$.

A number of articles reported the protection effect of silicon nitride film on electrical characteristics under total dose irradiation [11, 12].

The quantum effect should be taken into account when the device size down-scaling into the nanometer-level. The threshold surface potential of relaxed Si can be shown in Eq. (7)

$$\psi_{th,si} = 2\phi_B + \xi V_t + E_{g,dop} \tag{7}$$

where ϕ_B, V_t and $E_{g,dop}$ are the Femi potential, thermal voltage and band-gap narrowing, respectively. ξ is fitting parameter.

In order to derive the change of threshold surface potential ($\Delta\psi_{s,ssi}$) under the action of stress. With the quantum effects considering, the relationship of the inversion charge density and surface potential need to be modified as [13]:

$$Q_{inv,ssi} = \left(\frac{2qK_B T m_{d,0}}{\pi\hbar^2 N_A}\right)\left(\frac{n_{i,ssi}^2}{N_{C,ssi}}\right)\exp\left(\frac{E_{0,ssi}}{K_B T}\right)\exp\left(\frac{q\psi_{s,ssi}}{K_B T}\right) \tag{8}$$

where $m_{d,o}$ is the effective mass of states density of two-dimensional. $\psi_{s,ssi}$ is the surface potential under the action of stress. $n_{i,ssi}$, $N_{C,ssi}$ and $E_{0,ssi}$ are the intrinsic carrier concentration, effective states density of conduction band and the ground-state energy under the action of stress, respectively.

Using the condition of the inversion charge at the threshold point, which is

$$Q_{inv,si}(\psi_{th,si}) = Q_{inv,ssi}(\psi_{th,si} + \Delta\psi_{s,ssi}) \tag{9}$$

The change of surface potential $\Delta\psi_{s,ssi}$ can be obtained due to the stress effect, as shown in Eq. (10).

$$\Delta\psi_{s,ssi} = \left(\frac{\Delta E_{0,ssi} + \Delta E_{g,ssi}}{q}\right) + V_t \ln\left(\frac{N_{V,si}}{N_{V,ssi}}\right) + \frac{1}{2}V_t \ln\left[\frac{m_{t,\parallel}}{m_{t,\parallel}(\varepsilon)}\frac{m_{t,\perp}}{m_{t,\perp}(\varepsilon)}\right] \tag{10}$$

where $N_{V,si}$ and $N_{V,ssi}$ are the effective states density of valence band relaxation and strained Si, respectively. $m_{t,//}$ and $m_{t,\perp}$ are the effective mass of the parallel and

DOI: 10.1587/elex.14.20170411
Received April 21, 2017
Accepted April 28, 2017
Publicized May 17, 2017
Copyedited June 10, 2017

IEICE Electronics Express, Vol.14, No.11, 1–10

vertical, respectively. $\Delta E_{0,ssi}$ is the change of ground-state energy under the action of stress, which can be expressed as:

$$\Delta E_{0,ssi} = \Delta E_{C,\Delta Z} + [(E_{s,ssi})^{2/3} - (E_{s,si})^{2/3}]\left(\frac{9\pi q\hbar}{8\sqrt{2m_l}}\right)^{2/3} \quad (11)$$

where $\Delta E_{C,\Delta Z}$ is the conduction band shift of the ΔZ valley. $E_{s,ssi}$ and $E_{s,si}$ are the surface electric field with the stress and the without stress, respectively, which are:

$$E_{s,si} = \left(\frac{2qN_A\psi_{th,si}}{\varepsilon_{si}}\right)^{1/2}, \quad E_{s,ssi} = \left(\frac{2qN_A\psi_{th,ssi}}{\varepsilon_{si}}\right)^{1/2} \quad (12)$$

The one-dimensional equation of the surface potential can be obtained by Eqs. (10) (11) and (12).

$$\psi_{th,ssi} + A(\psi_{th,ssi})^{1/3} + B = 0 \quad (13)$$

Solving Eq. (13), we have $\psi_{th,ssi} = (\alpha + \beta)^3$, where

$$\alpha = [-(B/2) + \sqrt{(A/3)^3 + (B/2)^2}]^{1/3}, \quad (14)$$

$$\beta = [-(B/2) - \sqrt{(A/3)^3 + (B/2)^2}]^{1/3} \quad (15)$$

$$A = -\frac{1}{q}\left(\frac{9\pi q\hbar}{8\sqrt{2m_l}}\right)^{2/3}\left(\frac{2qN_A}{\varepsilon_{si}}\right)^{1/3} \quad (16)$$

$$B = -A(\psi_{th,si})^{1/3} - \psi_{th,si} - V_t \ln\left(\frac{N_{V,si}}{N_{V,ssi}}\right) - \frac{1}{2}V_t \ln\left[\frac{m_{t,\parallel}}{m_{t,\parallel}(\varepsilon)}\frac{m_{t,\perp}}{m_{t,\perp}(\varepsilon)}\right] - \left(\frac{\Delta E_{C,\Delta Z} + \Delta E_{g,\Delta Z}}{q}\right) \quad (17)$$

Before deducing threshold surface potential of two-dimensional, the effective doping concentration of the substrate and the maximum width of the depletion regions should be modified as [14]:

$$N_{A,eff} = N_A\left[1 - \left(\sqrt{1 + \frac{2W_{dv}}{R_j}} - 1\right)\frac{R_j}{L}\right] \quad W_{dv} = \sqrt{\frac{2\varepsilon_{si}\psi_{th,ssi}}{qN_A}} \quad (18)$$

A parameter of channel depletion width has been proposed by Suzuki [15]:

$$\kappa = \frac{1}{1 - 2\exp\left(-\frac{L}{\lambda}\right)} \quad (19)$$

The maximum width of the depletion-layer (W_d) and the average width of the depletion-layer W_{dv} are linked by this fitting parameter ($W_d = \kappa W_{dv}$) and $\lambda = 0.65(W_S + W_D)$, where

$$W_S = \sqrt{\frac{2\varepsilon_{si}}{q}\frac{N_D}{N_A}\left(\frac{\psi_{bi,si}}{N_D + N_A}\right)} \quad W_D = \sqrt{\frac{2\varepsilon_{si}}{q}\frac{N_D}{N_A}\left(\frac{\psi_{bi,si} + V_{DS}}{N_D + N_A}\right)} \quad (20)$$

where $\psi_{bi,si} = V_t \ln[N_A N_D/(n_{i,si})^2]$ is the built-in potential of source/drain-substrate. N_A and N_D are concentration of the source and drain region, respectively.

Oxide traps charge in the oxide layer and interface traps are induced by irradiation. Thus, the flat band voltage can be modified as:

DOI: 10.1587/elex.14.20170411
Received April 21, 2017
Accepted April 28, 2017
Publicized May 17, 2017
Copyedited June 10, 2017

IEICE Electronics Express, Vol.14, No.11, 1–10

$$V_{FB,ssi} = \left(\frac{\phi_M - \phi_{ssi}}{q}\right) - \frac{(Q_{ox} + qN_{ot} - qN_{it})}{C_{ox}} \tag{21}$$

where ϕ_M and ϕ_{ssi} are the work function of metal gate and the substrate of strained Si respectively. Q_{ox} and C_{ox} are the initial surface charge density and capacitance in the oxide layer respectively.

The work function of the substrate can be modified due to the strain effect.

$$\phi_{ssi} = \chi_{ssi} + E_{g,ssi}/2 + \phi_{fp,ssi}, \quad \chi_{ssi} = \chi_{si} + 0.57\sigma/7.55, \quad E_{gssi} = 1.12 - 0.0336\sigma$$

where σ is stress.

Due to the quantization effects, the peak density of the inversion charge is located in the strained silicon ΔZ away from the oxide/silicon interface. As a result, it is necessary to modify flat band voltage and the oxide thickness.

$$V_{FB,ssi} \rightarrow V_{FB,ssi} + qN_A\Delta Z\left(\frac{\Delta Z}{2\varepsilon_{si}} + \frac{t_{ox}}{\varepsilon_{ox}}\right), \quad t_{ox} \rightarrow t_{ox} + \frac{\varepsilon_{ox}}{\varepsilon_{si}}\Delta Z \tag{22}$$

where t_{ox}, ε_{ox} and ε_{si} are the oxide thickness, dielectric constant of the oxide layer and Si, respectively.

The two-dimensional Poisson's equation can be expressed as:

$$\frac{\partial^2\psi(x,y)}{\partial x^2} + \frac{\partial^2\psi(x,y)}{\partial y^2} = \frac{qN_{A,eff}}{\varepsilon_0\varepsilon_{si}} \tag{23}$$

The vertical component of the electrostatic potential can be approximated as:

$$\psi(x,y) = \psi_S(x) + C_1(x)y + C_2(x)y^2 + C_3(x)y^3 \tag{24}$$

The coefficients in (24) are determined from the boundary conditions, which can be described as:

$$\left[\frac{\partial\psi(x,y)}{\partial y}\right]_{y=0} = -\left(\frac{\varepsilon_0}{\varepsilon_{si}}\right)\left(\frac{V_{GS} - V_{FB} - \psi_S(x)}{t_{ox}}\right) \tag{25}$$

$$\psi(x, W_d) = 0, \quad \left[\frac{\partial\psi(x,y)}{\partial y}\right]_{y=W_d} = 0 \tag{26}$$

Then the coefficients of $C_1(x)$, $C_2(x)$ and $C_3(x)$ are obtained, and substituting these coefficients into Eq. (24):

$$\psi(x,y) = \psi_s(x) - \left[\frac{V_G - \psi_S(x)}{\gamma t_{ox}}\right]y + \left[\frac{3\gamma t_{ox} + 2W_d}{\gamma t_{ox}W_d^2}(V_G - \psi_S(x)) - \frac{3}{W_d^2}V_G\right]y^2 - \left[\frac{2\gamma t_{ox} + W_d}{\gamma t_{ox}W_d^3}(V_G - \psi_S(x)) - \frac{2}{W_d^2}V_G\right] \tag{27}$$

where $\gamma = \varepsilon_{si}/\varepsilon_{ox}$, $V_G = V_{GS} - V_{FB,ssi}$ is effective voltage. Boundary conditions:

$$\psi_s(0) = \psi_{bi,ssi} \text{ and } \psi_s(L) = \psi_{bi,ssi} + V_{DS}.$$

where $\psi_{bi,ssi} = V_t \ln[N_AN_D/(n_{i,ssi})^2]$ is the build-in junction potential.

Substituting Eq. (27) into Eq. (23), and setting y = 0, thus the surface potential is given by:

$$\psi_s(x) = V_G - \left(\frac{qN_{A,eff}}{\varepsilon_{si}} + \frac{6}{W_d^2}V_G\right) \times l^2 + \zeta(x) \tag{28}$$

where l is commonly referred to as the characteristics scaling length and is given by:

DOI: 10.1587/elex.14.20170411
Received April 21, 2017
Accepted April 28, 2017
Publicized May 17, 2017
Copyedited June 10, 2017

IEICE Electronics Express, Vol.14, No.11, 1–10

$$l = [\gamma t_{ox} W_d^2/2(3\gamma t_{ox} + 2W_d)]^{1/2} \text{ and } \zeta(x) = \frac{\zeta_1 \sinh\left(\frac{L-x}{l}\right) + \zeta_2 \sinh\left(\frac{L}{l}\right)}{\sinh\left(\frac{L}{l}\right)}$$

$$\zeta_1 = \psi_{bi,ssi} - V_G + \left(\frac{qN_{A,eff}}{\varepsilon_{si}} + \frac{6}{W_d^2} V_G\right) \times l^2,$$

$$\zeta_2 = \psi_{bi,ssi} + V_{DS} - V_G + \left(\frac{qN_{A,eff}}{\varepsilon_{si}} + \frac{6}{W_d^2} V_G\right) \times l^2$$

In most of the measurement of threshold voltage, surface potential is symmetric in the channel, the minimum surface potential is located in the middle of the channel, and setting x = L/2 [16] in Eq. (28). In this operation, Eq. (28) should be rewritten as:

$$\psi_{s,\min} \approx V_G - \left(\frac{qN_{A,eff}}{\varepsilon_{si}} + \frac{6}{W_d^2} V_G\right) \times l^2 + (\zeta_1 + \zeta_2) \frac{\sinh\left(\frac{L}{2l}\right)}{\sinh\left(\frac{L}{l}\right)} \tag{29}$$

when the $\psi_{s,\min}$ achieves one-dimensional potential of Eq. (13), the device starts to work.

In addition, the band-narrowing effect and the DIBL effect also need to be considered. From Eqs. (13) and (29), the (2D) threshold voltage model of the uniaxial strained Si nanometer NMOSFETS devices after considering the quantum effect and total dose radiation effect is calculated by:

$$V_{th,ssi} = V_{FB,ssi} - V_{DIBL} + \frac{\psi_{th,ssi} + \left[1 - 2\frac{\sinh\left(\frac{L}{2l}\right)}{\sinh\left(\frac{L}{l}\right)}\right] \frac{qN_{A,eff}}{\varepsilon_{si}} l^2 - \frac{\sinh\left(\frac{L}{2l}\right)}{\sinh\left(\frac{L}{l}\right)} (2\psi_{bi,ssi} + V_{DS})}{\left[1 - 2\frac{\sinh\left(\frac{L}{2l}\right)}{\sinh\left(\frac{L}{l}\right)}\right] \left[1 - \frac{6}{W_d^2} l^2\right]} \tag{30}$$

3 Experiment

The device of uniaxial strained Si nanometer NMOSTET were irradiated with ^{60}Co γ-ray at a dose rate of 29 rad (SiO_2)/s at room temperature, with a gate bias of 1 V. Device parameters were measured in the dose range from 0.5 kGy to 2.5 kGy, using an HP4155B parametric analyzer. Irradiation bias: $V_G = 1$ V, drain voltage V_D is equal to source voltage V_S ($V_D = V_S = 0$). Measurement bias: $V_G = 0$–1 V, scanning voltage $V_{step} = 0.05$ V, $V_D = 50$ mv, $V_S = 0$ V. Fig. 2(a) is the micrograph of a uniaxial strained Si nanometer NMOSTET device. TiAl material is used for the gate electrode. The oxide layer is SiO_2 and HfO_2, the equivalent oxide thickness being 1 nm. The junction depth of source/drain region is 25 nm and the gate length is 50 nm. Fig. 2(b) is schematic cross-section of uniaxial strained Si nanometer

DOI: 10.1587/elex.14.20170411
Received April 21, 2017
Accepted April 28, 2017
Publicized May 17, 2017
Copyedited June 10, 2017

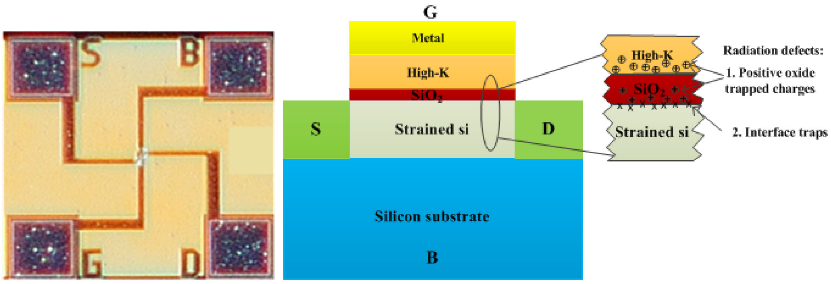

(a) (b)

Fig. 2. (a) Micrograph of uniaxial strained Si nanometer NMOSFET device and (b) Schematic cross-section of uniaxial strained Si nanometer NMOSFET indicating the buildup of radiation-induced oxide trapped charge and the generation of interface traps.

NMOSFET indicating the buildup of radiation-induced oxide trapped charge and the generation of interface traps.

The V_{th} shifts of relaxed nanometer Si NMOSFET and uniaxial strained Si nanometer NMOSFET device with different absorbed doses are listed in Table I. As can be seen from the Table I, the V_{th} drift of relaxed Si nanometer NMOSFET is similar to that of uniaxial strained Si nanometer NMOSFET. It can be inferred that the stress does not change when compared with the case before irradiation, and the experimental results are in good agreement with the previous reports [12].

Table I. The V_{th} shift of relaxation and uniaxial strained Si nanometer NMOSFET device under the absorbed dose.

Dose/KGy	0.5	1.0	1.5	2.0	2.5
$\Delta V_{th,si}/V$	−0.0352	−0.0403	−0.0410	−0.0415	−0.0431
$\Delta V_{th,ssi}/V$	−0.0354	−0.0405	−0.0408	−0.0417	−0.0428

4 Results and discussion

A two-dimensional analytical model of threshold voltage (V_{th}) has been developed with the degradation due to the total dose irradiation taken into consideration, and numerical simulations are implemented by Matlab. Partial model parameters are summarized in Table II.

Depicted in Fig. 3 is the variation of V_{th} with irradiation dose for (a) different junction depth ($R_j = 25$ nm and $R_j = 50$ nm) of source/drain region and (b) different channel length. As can be seen from Fig. 3(a), the effective doping concentration (Eq. 18) in the channel decreases with increased junction depth of the source/drain region, so that the device is easier to open and V_{th} decreases slightly. From Fig. 3(b), as the channel length decreases, V_{th} decreases due to the short channel effect. The depletion regions of source and drain are seriously overlapped, and more charge sharing appears in these two regions, which diminishes the ability of gate control. Obviously, the variation of V_{th} shift on irradiation dose is hardly different among different junction depths or channel lengths. Moreover, the

DOI: 10.1587/elex.14.20170411
Received April 21, 2017
Accepted April 28, 2017
Publicized May 17, 2017
Copyedited June 10, 2017

Table II. Summary of partial model parameters for uniaxial strained Si nano NMOSFET.

Parameter	Description	Value	Unit
T	Temperature	300	K
W	Gate width	3	um
L	Gate length	50	nm
N_D	Doping concentration of source	$2 * 10^{19}$	cm^{-3}
N_D	Doping concentration of drain	$2 * 10^{19}$	cm^{-3}
k_g	Electron-hole pairs	$8.1 * 10^{10}$	$cm^{-3}.Gy^{-1}$
$N_{Si\text{-}H}$	Silicon dangling bond density of hydrogen passivation	$4.8 * 10^{12}$	cm^{-2}
σ_{DH}	Trapped cross section of holes with hydrogen traps	$2.0 * 10^{-11}$	cm^{-2}
Q_{ox}	Initial charge surface density	$0.4 * 10^{11}$	cm^{-2}
N_t	Hole trap concentration	$8.0 * 10^{15}$	cm^{-2}
N_A	Doping concentration of substrate	$2 * 10^{18}$	cm^{-3}
ε_{si}	Silicon relative dielectric constant	11.9(Si)	—

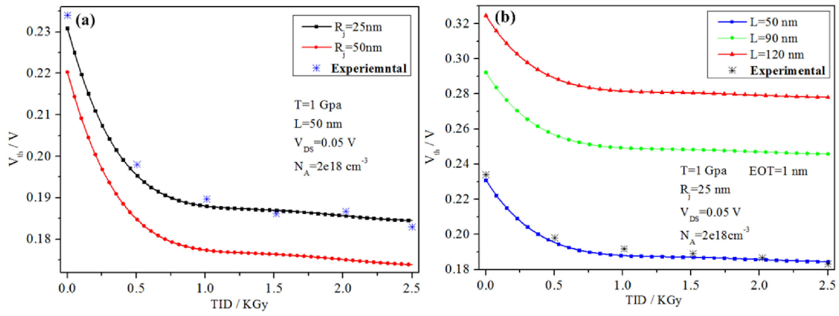

Fig. 3. The relationship of V_{th} with irradiation dose for (a) junction depth and (b) the channel length.

calculation results from the model are consistent with the experimental data, indicating the validity of our proposed model.

Fig. 4 shows V_{th} versus irradiation dose for different oxide parameters ((a) dielectric (b) thickness). As shown in Fig. 4(a), the V_{th} shift for the gate dielectric of SiO_2 ($\varepsilon_f = 3.9$) is larger than that of HfO_2 ($\varepsilon_f = 25$) and Al_2O_3 ($\varepsilon_f = 11$). The larger the permittivity of the gate dielectric, the smaller the variation of threshold voltage with increasing irradiation dose. In Fig. 4(b), apparently, the thicker the oxide layer, the more holes are captured, which decreases the V_{th}. The V_{th} shift increases sharply as the thickness of gate oxide increases slightly under the total irradiation dose, which indicates that the oxide thickness is very sensitive to the irradiation effect.

The relationship of V_{th} with the irradiation dose for (a) different gate voltages and (b) stress are shown in Fig. 5. As can be seen from Fig. 5(a), V_{th} decreases with the increasing irradiation dose due to more trapped holes in the oxide layer. A higher gate bias can also increase the electric field force that can trap more holes, thus reducing the V_{th}. Fig. 5(b) shows the increase of stress leads to the narrowing

DOI: 10.1587/elex.14.20170411
Received April 21, 2017
Accepted April 28, 2017
Publicized May 17, 2017
Copyedited June 10, 2017

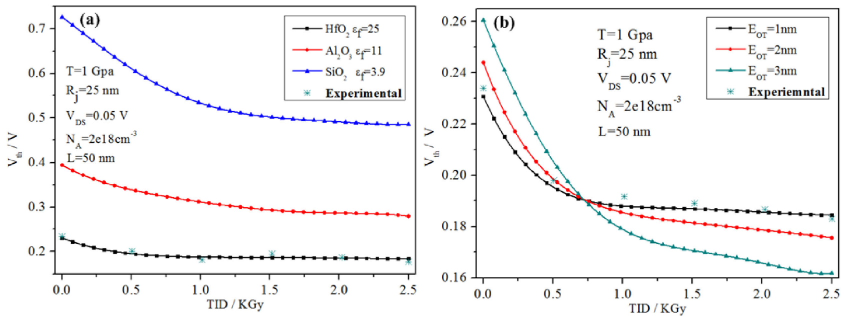

Fig. 4. The relationship of V_{th} with irradiation dose for oxide parameters dielectric constant (a) and thickness (b).

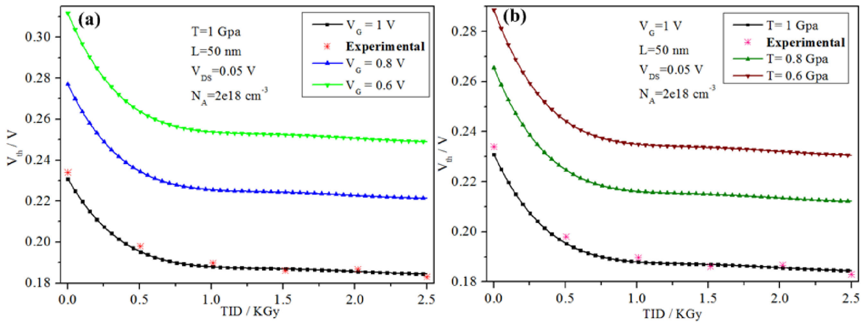

Fig. 5. The variation of V_{th} with irradiation dose for (a) different gate voltages and (b) stress.

of band gap and the decreasing of flat band voltage, which reduces the V_{th}. Good agreement between experiments and simulations are demonstrated.

5 Conclusion

A two-dimensional analytic model on V_{th} of uniaxial strained Si nanometer NMOSFET was established due to the total dose irradiation. Moreover, the results from the model are compared with the experimental data and they are found to be in good agreement. Thus, the proposed model provides good reference for research on irradiation reliability and application of strained integrated circuit of uniaxial strained Si nanometer n-channel metal-oxide-semiconductor field-effect transistor.

Acknowledgements

This work was supported by the National Natural Science Foundation of China (Grant No. 61474085) and the Science Research Plan in Shaanxi Province, China (Grant No. 2016GY-085).

DOI: 10.1587/elex.14.20170411
Received April 21, 2017
Accepted April 28, 2017
Publicized May 17, 2017
Copyedited June 10, 2017